

N. Hansen, N. Gaiser, T. Bierkandt, P. Oßwald, M. Köhler, J. Zádor, P. Hemberger, Identification of Dihydropentalenes as Products of the Molecular-Weight Growth Reaction of Cyclopentadienyl Plus Propargyl, *J. Phys. Chem. A* 129 (2025) 1714-1725.

This document is the Accepted Manuscript version of a Published Work that appeared in final form in *The Journal of Physical Chemistry A*, copyright © American Chemical Society after peer review and technical editing by the publisher. To access the final edited and published work see <https://doi.org/10.1021/acs.jpca.4c06549>.

**Identification of Dihydropentalenes as Products of the Molecular-Weight
Growth Reaction of Cyclopentadienyl plus Propargyl**

Nils Hansen^{a,*}, Nina Gaiser^b, Thomas Bierkandt^b, Patrick Oßwald^b, Markus Köhler^b,
Judit Zádor^a, Patrick Hemberger^c

^a*Combustion Research Facility, Sandia National Laboratories, Livermore, California 94551,
USA*

^b*German Aerospace Center (DLR), Institute of Combustion Technology, 70569 Stuttgart,
Germany*

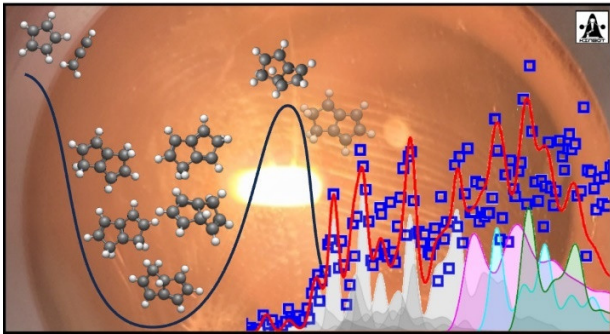
^c*Laboratory for Synchrotron Radiation and Femtochemistry, Paul Scherrer Institute (PSI), 5232
Villigen, Switzerland*

to be submitted to:

J. Phys. Chem. A (A. M. Wodtke Festschrift)

Supplementary Information is included.

Table-Of-Contents Graph:



ABSTRACT

The resonance-stabilized cyclopentadienyl (C_5H_5) and propargyl (C_3H_3) radicals are important precursors for polycyclic aromatic hydrocarbons (PAHs) and thus play a significant role in molecular-weight growth and soot formation processes under combustion conditions. In this work, we describe an experimental and theoretical investigation of the $C_5H_5 + C_3H_3$ reaction. Experimentally, we studied this reaction in a resistively heated microtubular SiC reactor at a controlled temperature of ~ 1150 K and a pressure near 10-20 Torr. The reactants C_5H_5 and C_3H_3 were pyrolytically generated from anisole ($C_6H_5OCH_3$) and propargyl bromide (C_3H_3Br). We identified the reactants and the C_8H_8 products isomer-selectively utilizing photoion mass-selected threshold photoelectron spectroscopy (ms-TPES). The experimentally observed predominant formation of dihydropentalenes over the ring-enlargement reaction to styrene is consistent with our theoretical predictions of the kinetics on the newly calculated C_8H_8 potential energy surface. This work highlights dihydropentalenes as reactants in molecular-weight growth reactions and as potential building blocks in versatile routes for the formation of curved PAHs.

KEYWORDS: polycyclic aromatic hydrocarbons (PAHs); molecular-weight growth; cyclopentadienyl; propargyl; threshold photoelectron spectroscopy (TPES); automated chemical kinetics

1. Introduction

Understanding the physical chemistry of molecular-weight growth responsible for the formation of polycyclic aromatic hydrocarbons (PAHs) in extreme conditions, such as combustion and astrochemical environments, remains an intriguing topic.¹⁻⁵ It is understood that PAHs are formed as a result of incomplete combustion processes and serve as precursors of soot particles. Once released to the atmosphere, PAHs have negative impacts on the environment and human health.⁶ Additionally, soot and PAHs serve as nucleation core in aviation-introduced contrail and subsequent cirrus cloud formation that was found to have a significant impact on climate warming due to radiative forcing.^{8,9}

Molecular-weight growth towards PAHs starts with the formation of the so-called “first aromatic ring” – typically, but not exclusively, benzene (C_6H_6) or phenyl (C_6H_5) which are formed through radical-radical and radical-molecule reactions.^{2,3,10} The key role of resonantly stabilized radicals, such as propargyl (C_3H_3),¹¹⁻¹³ allyl (C_3H_5),^{14,15} *i*- C_4H_5 ,¹⁶⁻¹⁸ and cyclopentadienyl (C_5H_5)^{19,20} is now well established and can be traced back to these radicals accumulating in high concentrations in flames. Especially the propargyl radical is prominently important in aromatics formation. Under most conditions, the reaction of two propargyl radicals has been identified as the main source of benzene/phenyl, the simplest aromatic ring structures. Propargyl reactions also contribute to the formation of larger species. For example, it is known that propargyl radicals can contribute to the formation of five-membered ring structures via aliphatically substituted aromatic rings.²¹⁻²⁶

The resonance-stabilized cyclopentadienyl radical plays a fascinating role in PAH formation chemistry. On one hand it can be formed through the propargyl + C_2H_2 reaction, and then contribute to molecular-weight growth via reactions with other radicals or molecules.²⁷⁻³² On the other hand, C_5H_5 decomposes to C_3H_3 and C_2H_2 at high, combustion-relevant, temperatures,^{33,34}

thus limiting the importance of C₅H₅ in molecular-weight growth. Under flame conditions, we found C₅H₅ chemistry only to be important when the fuel contained a five-membered ring or when such a ring is readily formed through fuel decomposition.^{20, 35, 36}

Most importantly, C₅H₅ can undergo ring-enlargement reactions, also known as ring-expansion reactions, that convert the five-membered ring structure into a six-membered ring. A typical example is the C₅H₅ + CH₃ reaction that, via fulvene as an intermediate, can lead to benzene + 2H.^{19, 20, 37} In an analogous reaction with a methyl radical, indenyl can be transformed into naphthalene.³⁸ Ring-enlargement reactions of C₅H₅ radicals with C₂ and larger species are of particular interest, because these reactions bypass benzene as the “first aromatic ring” and form heavier aromatics directly.^{29, 39} A typical example is the reaction of C₅H₅ with acetylene forming benzyl radicals (and/or tropylium) or its self-recombination reaction that leads to naphthalene.^{19, 40, 41}

The cross reaction of cyclopentadienyl with propargyl radicals



has been studied theoretically by Sharma *et al.*⁴² using CBS-QB3 theory. Their chemistry modeling work of methane flames doped with 1,3-, 2,4-, and 1,4-hexadiene showed that reaction (R1) contributes through a ring-enlargement reaction to the formation of styrene (C₆H₅-CH=CH₂), the most stable isomeric form of C₈H₈. According to their work, the reaction proceeds through various cyclopentadienyl-substituted allene and propyne isomers. Prior theoretical and experimental work on C₈H₈ pyrolysis and isomerization also highlights the importance of isomers such as cyclooctatetraene, different dihydropentalene isomers, cardene (benzocyclobutane), semibullvalene, barrelene, and decomposition products such as benzene + acetylene or *o*-benzyne + ethylene.⁴³⁻⁴⁹ For the readers' convenience, some C₈H₈ isomers, including the high-energy cubane, are illustrated in Figure 1.

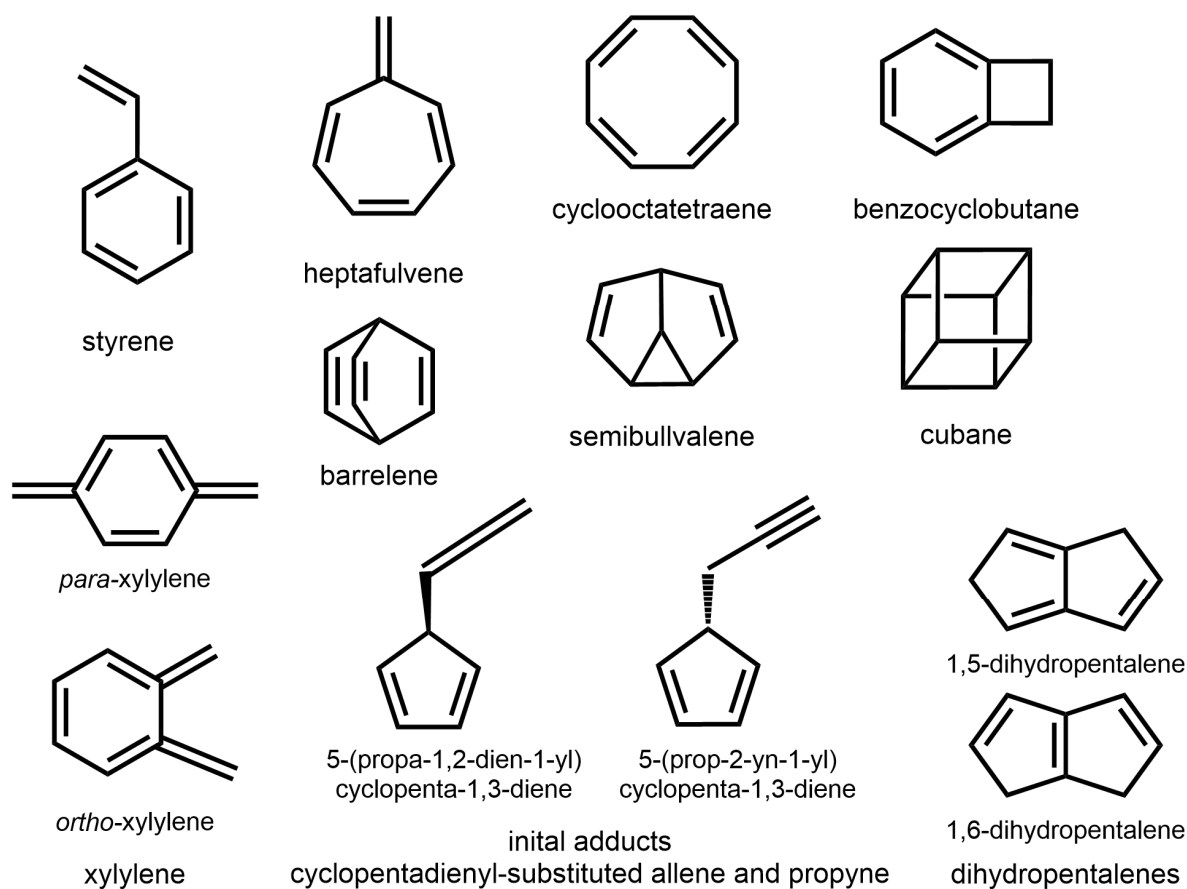


Figure 1: Visualization of a few C_8H_8 isomers.

The dihydropentalenes (DHPs) are of particular interest for the work described here, given that a product analysis of similar propargyl radical reactions,^{21, 23, 24, 26} suggests the possibility that the formation of styrene in reaction (R1) competes with ring-closure reactions that would lead to dihydropentalene structures. Both pathways, the ring-enlargement and cyclization steps, are summarized in Figure 2.

In this work, we used a combination of isomer-selective species measurements at the exit of a microtubular reactor in conjunction with a theoretical exploration of the C_8H_8 potential energy surface to investigate reaction (R1) at an unprecedented detail. Using flash pyrolysis, we generated C_5H_5 and C_3H_3 radicals *in-situ* and analyzed the reaction intermediates and products with mass-

selected threshold photoelectron spectroscopy (ms-TPES).^{50, 51} This approach uses a unique tool for product detection and isomer-specific identification in reactive environments. In combination with theoretical calculations of the C₈H₈ potential energy surface using the automated workflow code Kinbot,^{52, 53} we identified various C₈H₈ isomers as intermediates and products of reaction (R1), including dihydropentalene isomers.

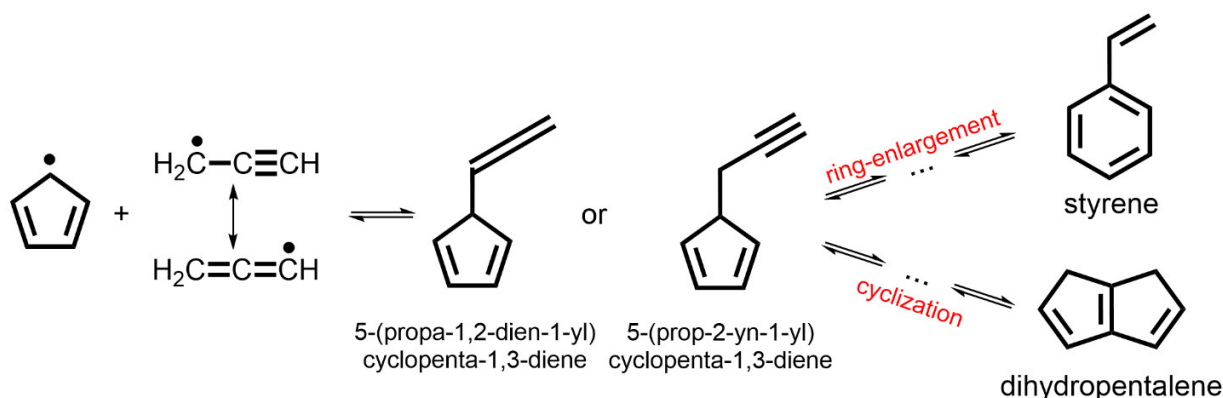
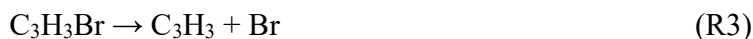


Figure 2: Graphical summary of potential C₅H₅ + C₃H₃ reaction pathways. Following the initial adduct formation, styrene, the most stable C₈H₈ isomer, and dihydropentalenes can be formed through ring-enlargement and cyclization reactions, respectively.

2. Experimental Methods

Similar to our earlier experiments on radical-radical chemistry,^{21, 22, 54-57} we generated the reactants through flash pyrolysis in a resistively heated SiC microtubular reactor⁵⁸ (1 mm ID, 35-40 mm long) at ca. 1150 K and 10-20 mbar to follow their reactions and to identify the main

intermediates and products. In this work, anisole ($C_6H_5OCH_3$) and propargyl bromide (C_3H_3Br) served as precursors for C_5H_5 and C_3H_3 , respectively:



The pyrolysis conditions were chosen to maximize production of C_5H_5 and C_3H_3 , thus, to optimize bimolecular reactions. The pyrolysis temperature was controlled by the heating power and a previously determined power-temperature calibration (based on a type-c thermocouple measurement on the outside wall of the reactor) was used as a temperature measurement.²²

The results presented in this paper were recorded at a pyrolysis temperature of 1150 K, at which both precursors make the desired reactants efficiently, as traced by the temperature dependent ion signal. By flowing argon over the liquid precursors, anisole and propargyl bromide were added to the gas stream according to their vapor pressures. The liquid precursors were kept at room temperature for the duration of the experiments. The flows were varied independently to achieve the targeted optimal conversion (5 sccm through the anisole and 0.5 sccm through the C_3H_3Br precursors and an additional argon stream of 30 sccm), leading to a total gas-stream of 35.5 sccm with about 1% of each precursor. The inlet pressure was about 100 mbar and fluid dynamics simulation can be used to simulate the pressure in the reactor.^{54, 59}

The reaction mixture was expanded into high vacuum to form an effusive molecular beam and was analyzed using the CRF-PEPICO spectrometer that combines a time-of-flight mass spectrometer and a velocity map imaging photoelectron spectrometer.⁶⁰ Ions and electrons were

collected in delayed coincidence, permitting to record photoion mass-selected threshold photoelectron spectra (ms-TPES).⁶¹

These spectra were recorded at the vacuum-ultraviolet (VUV) beamline of the Swiss Light Source (SLS) at the Paul Scherrer Institute (PSI). A detailed description of the beamline is given in Ref. [62]. In short, synchrotron radiation was provided by a bending magnet, collimated and diffracted by a plane grating ($150 \text{ grooves} \cdot \text{mm}^{-1}$) with a resolving power of 1500. Higher harmonic radiation was suppressed in a rare gas filter operated with an Ar/Ne/Kr mixture at a pressure of 10 mbar. The photon energy was scanned in 10 meV steps and calibrated using autoionization resonances in Ar. For the analysis, threshold electrons were selected with an energy resolution of 5-7 meV and contributions of hot background electrons and false coincidences were subtracted.⁶³

64

3. Computational Methods

3.1 Potential Energy Surface Exploration

We used our automated chemical kinetics workflow software, KinBot,^{52, 53} to characterize the C_8H_8 potential energy surface (PES) systematically. KinBot initiates the exploration from a structure provided by the user, which in this case was 5-(propa-1,2-dien-1-yl)cyclopenta-1,3-diene, one of the adducts formed when cyclopentadienyl and propargyl react (see Figs 1 and 2). In general, it does not matter which well we use to initiate the search. We could have used any other well, but it makes sense for our application to start in a well that is formed readily in the targeted reaction.

We activated all reaction templates of KinBot and extended them with a new one. Previously, only 1,2- H_2 -elimination reactions were considered. Now, we generalized this template for distant

carbons as well (1,3, 1,4, etc.). Many of the structures on the PES feature rigid backbone motifs, *e.g.*, consecutive double bonds. We limited the search across such motives up to 5 Å to cut down on searches that most certainly will lead to too high energy pathways. Each reaction template defines important internal coordinates and their values that are expected to bring the reactant in the vicinity of a first-order saddle point, which were then optimized to a true saddle. A reaction pathway is considered valid if its energy is below a user-defined threshold and if a distinct product is detected by using intrinsic reaction coordinate (IRC) calculations. If the product is a new well, the search continues until no new wells are found. KinBot used L1=B3LYP/6-31+G for the reaction search with a 58.5 kcal/mol threshold above the initial structure. This threshold was determined by inspecting the pathways stemming from this well all the way to styrene.⁴² Possible homolytic scission reactions were also detected based on the energy of the bimolecular asymptotes, which was allowed to be as high as 63.5 kcal/mol to account for the looseness of the related transition states.

For each valid stationary point KinBot carried out a conformational search on a 120-degree grid up to four conformer-generating dihedrals (max. $3^4=81$ conformers). No structure we found had more than this. Ring conformers were sampled as described in Ref. [65]. The lowest energy structures were refined at the L2= ω B97X-D/6-311++G** level, and single point energies were calculated at L3=CCSD(T)-F12a/cc-pVnZ-F12, $n= D, T$ (denoted as L3_D and L3_T). The L1 and L2 calculations were done using the Gaussian 16 suite,⁶⁶ while the L3 calculations were done in Molpro 2022.⁶⁷ The resulting PES was visualized and analyzed using the PESViewer tool,⁶⁸ and a selected set of microcanonical rate coefficients were calculated using MESS.^{69, 70}

3.2 Threshold-Photoelectron Spectra Simulation and Franck Condon spectral modeling

In the absence of reference data, the photoion mass-selected threshold photoelectron spectra were simulated by utilizing Franck-Condon spectral modeling. For these calculations, the geometries and force constant matrices of the neutral and cationic species were obtained at the B3LYP/6-311G++(d,p) levels of theory using Gaussian 16 (rev. C.02).⁶⁶ Franck-Condon stick spectra were calculated at 300 K utilizing ezSpectrum or Gaussian 16 and were subsequently convoluted with 20-50 meV full width half maximum (fwhm) Gaussian functions to fit the rotational envelope. The simulated spectra were shifted in the energy axis to fit the experimental ones and evaluated by G4 calculated adiabatic ionization energies (AIE_{calc}) to be within a range of $< \pm 80$ meV of the fundamental transition from the neutral into the cation.

4. Results and discussion

In a multi-step process, we analyzed photoionization mass spectra, threshold photoelectron spectra, and results from theoretical calculations of the C_8H_8 potential energy surface to gain important chemical insights into the kinetics of reaction (R1), the $C_5H_5 + C_3H_3$ reaction. The analysis is described next.

4.1 Overview Mass Spectra

In a first step, we recorded photoionization mass spectra to ensure that the reactants cyclopentadienyl (C_5H_5) and propargyl (C_3H_3) are formed cleanly in the flash pyrolysis and that the targeted C_8H_8 products are not formed in the pyrolysis of their perspective precursors, anisole and propargyl bromide. As part of this step, we also recorded photoionization mass spectra to ensure that the C_8H_8 is produced in the $C_5H_5 + C_3H_3$ cross reaction in detectable amounts. To this

end, Fig. 3 shows the sampled mass spectra after flash pyrolysis of (a) anisole ($C_6H_5OCH_3$), (b) propargyl bromide (C_3H_3Br), and (c) their mixture. The photon energies used here to acquire the overview mass spectra are chosen to be above the ionization energies of the targeted species (C_3H_3 , C_5H_5 , and C_8H_8 isomers), while trying to avoid, or at least minimize dissociative photoionization.

As known from previous work,⁷¹⁻⁷⁴ Figure 3(a) confirms that C_5H_5 is the main intermediate in the flash pyrolysis of anisole. We also detected a smaller amount of $C_5H_5CH_3$ isomers (methyl-

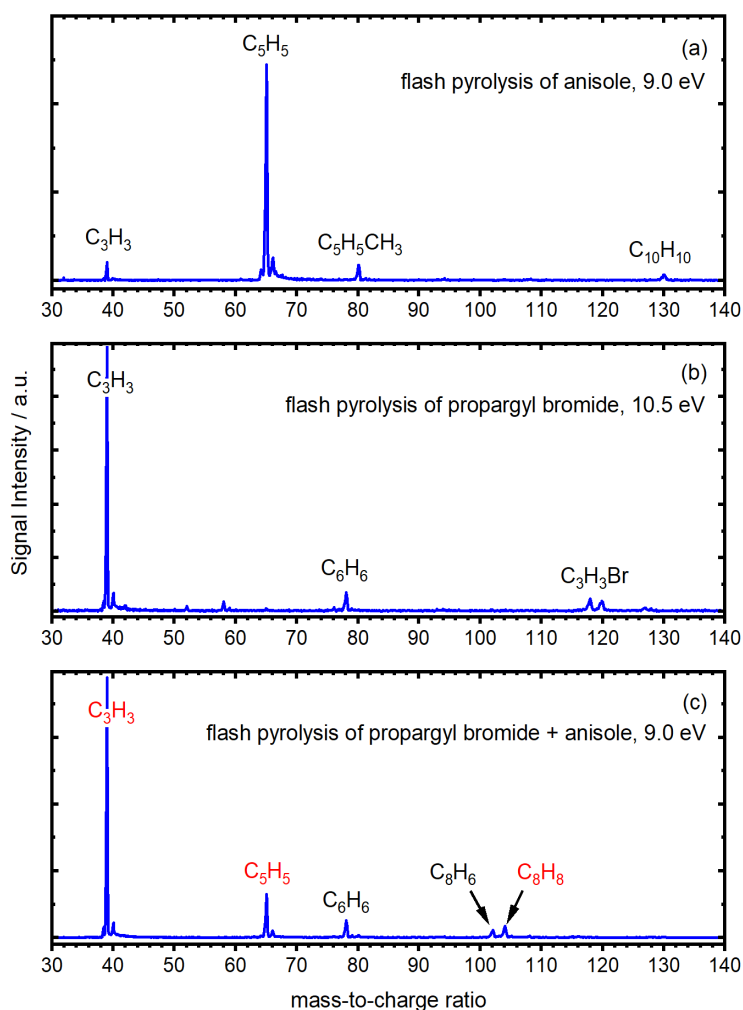


Figure 3: The experimentally observed mass spectra after flash pyrolysis of (a) anisole ($C_6H_5OCH_3$) and (b) propargyl bromide (C_3H_3Br). The spectra were recorded at 9.0 and 10.5 eV, respectively, at a temperature of ~ 1150 K, and a pressure of ~ 20 Torr. (c) Mass spectrum of the species exiting the microtubular reactor. The reactants (C_5H_5 and C_3H_3) and the C_8H_8 product are highlighted in red. The absence of the C_8H_8 signal in the two control experiments shown in (a) and (b) provides evidence for the observed C_8H_8 to result from the cross reaction of cyclopentadienyl with propargyl.

cyclopentadienes), a well-known intermediate in anisole pyrolysis.⁷⁵ C_3H_3 and $C_{10}H_{10}$ are decomposition and self-recombination products of cyclopentadienyl, respectively.^{19, 33} The absence of anisole, which has an ionization energy of 8.2 eV,⁷⁶ in the mass spectra that was recorded at 9.0 eV indicates that anisole is fully converted at these flash pyrolysis conditions.

At a photon energy of 10.5 eV (Fig. 3(b)) we detect C_3H_3 and C_6H_6 as intermediates and products in the flash pyrolysis of C_3H_3Br . At this photon energy, the precursor remains visible at $m/z = 118$ and 120, corresponding to the $C_3H_3^{79}Br$ and $C_3H_3^{81}Br$ isotopologues. C_6H_6 is a well-known reaction product of the $C_3H_3 + C_3H_3$ self-recombination.^{11, 12}

While the observation of these peaks already hints at the identity of the $m/z = 39$ and the $m/z = 65$ peaks as propargyl and cyclopentadienyl, a more rigorous identification based on the unique threshold photoelectron spectra is provided in the Supplementary Information.

Most importantly, both mass spectra in Fig. 3(a) and (b) indicate that C_8H_8 is not a product or intermediate of the flash pyrolysis of propargyl bromide or anisole. Because C_8H_8 is detectable only in the combined pyrolysis of propargyl bromide and anisole, we are confident that this observed C_8H_8 is a product of the targeted reaction (R1), the $C_5H_5 + C_3H_3$ reaction. No obvious reaction pathways of any pyrolysis byproducts are able to form C_8H_8 . The respective mass spectrum is shown in Fig. 3(c). Besides the C_8H_8 product, a mass peak for C_8H_6 is observed, which is only slightly less prominent than the C_8H_8 . Because the formation chemistry of C_8H_6 is not the subject of this study, we refrain from discussing C_8H_6 here in detail. In short, C_8H_6 is likely a product of C_8H_8 dehydrogenation that can occur at elevated temperatures either through sequential H-atom loss or direct H_2 elimination.

4.2 The C_8H_8 potential energy surface

With the detection of the closed-shell species with a molecular formula of C_8H_8 ($m/z = 104$), we shift our focus to the elucidation of its structural isomers. Based on the previous discussion, we can safely conclude that C_8H_8 is a direct product of reaction (R1), the $C_5H_5 + C_3H_3$ reaction. Before discussing the photoion mass-selective threshold photoelectron spectrum for $m/z = 104$ (C_8H_8) in detail, we will turn to the C_8H_8 potential energy surface that governs this reaction.

First, we start our discussion with a brief overview of the potential energy surface, to ensure that no pathways connecting large regions of the PES are overlooked.⁴¹ Second, we present the important pathways relevant for cyclopentadienyl + propargyl, reaction (R1). The C_8H_8 system is an extremely rich chemical landscape, and its complete characterization is beyond the scope of this work.

Using the automated tool KinBot, we found almost 400 wells in the prescribed energy range, and first briefly discuss them at the L3_D level. As mentioned before, the deepest well is styrene (0.0 kcal/mol) – see Fig. 1 for chemical structures. The next lowest energy structure is cardene (benzocyclobutane) at 12.3 kcal/mol above styrene. The next structure is *para*-xylylene at 17.5 kcal/mol, followed by the dihydropentalenes (19.9-28.7 kcal/mol), *ortho*-xylylene (23.8 kcal/mol), and heptafulvene (27.7 kcal/mol). Most of the rest of the C_8H_8 structures are densely populating the energy ladder, many of them are within 1 kcal/mol of their lower and higher energy neighbors, which highlights the challenges of any intuition-based exploration: it is simply impossible to predict which parts of this complex landscape are going to dominate without a systematic search and analysis. In addition to the wells, we also identified 32 bimolecular product

channels. The lowest energy one is benzene + acetylene at 37.5 kcal/mol, whereas cyclopentadienyl + propargyl is at 109.6 kcal/mol, making it a relatively high-energy entry point.

To interpret this large chemical space, we selected a core set of species relevant for this work, *i.e.*, the initial adduct, 1,5-dihydropentalene, cyclooctatetraene, barrelene and styrene, and used tools implemented in PESViewer to systematically find all important exits and lowest energy connections. More details about the selection process can be found in the SI. The simplified PES obtained in this manner for the title reaction is shown in Fig. 4 and can also be viewed in the SI as an interactive graph. It contains 20 wells and 8 bimolecular products with energies evaluated at the L3_T level.

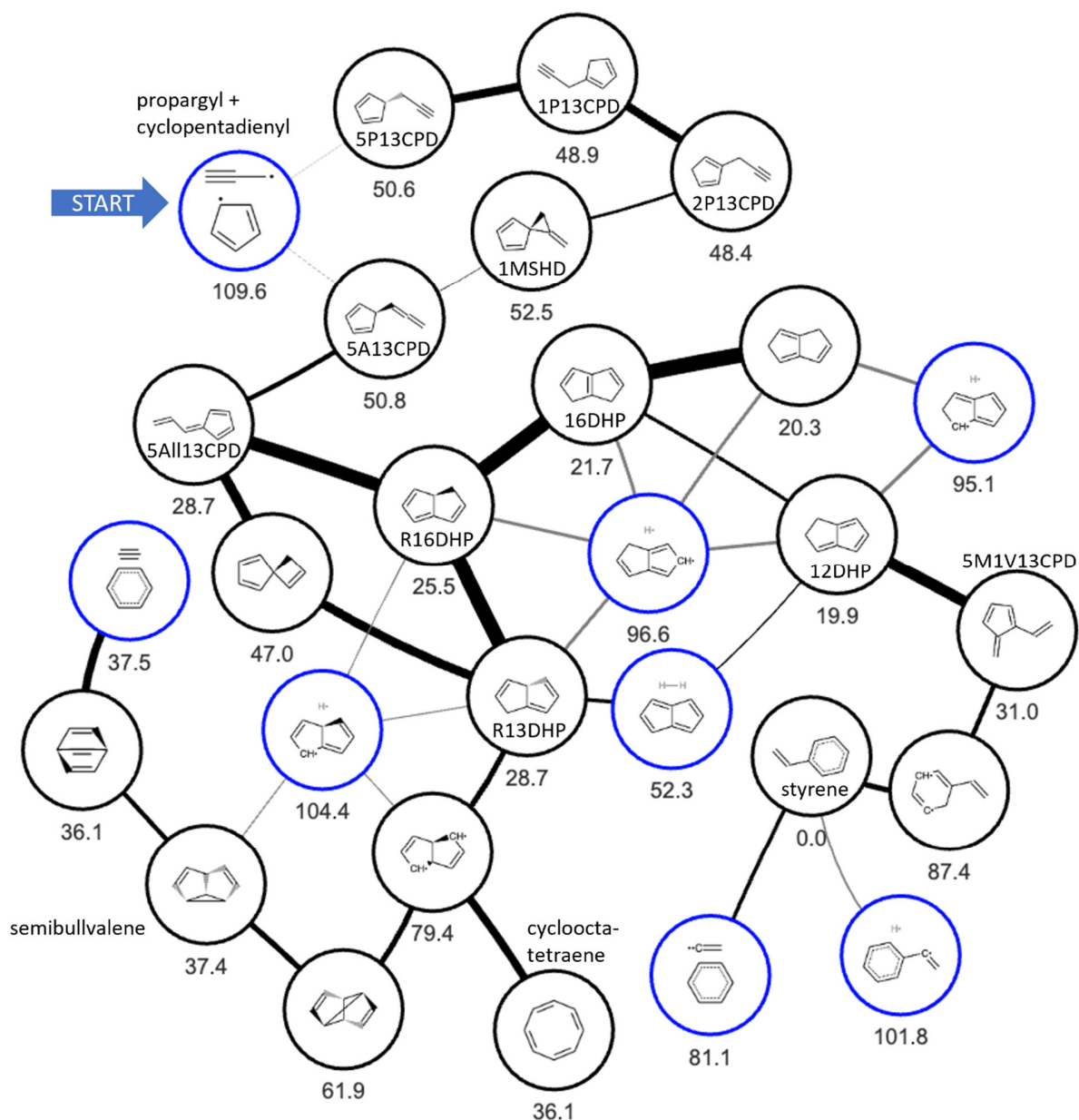


Figure 4: The network of reactions relevant for the cyclopentadienyl + propargyl entrance. Wells are circled with black, while bimolecular products with blue. Thicker edges represent lower barriers, and gray edges represent barrierless reactions. Well energies are shown in kcal/mol at the $L3_T$ level of theory relative to styrene and include ZPE. The figure is shown in the SI as an interactive graph.

Figure 5 shows the overall lowest energy pathway from cyclopentadienyl (C_5H_5) + propargyl (C_3H_3) to styrene, which features a >10 kcal/mol lower bottleneck barrier than the pathway described by Sharma *et al.*⁴² (also found by KinBot, see SI). The newly characterized path toward

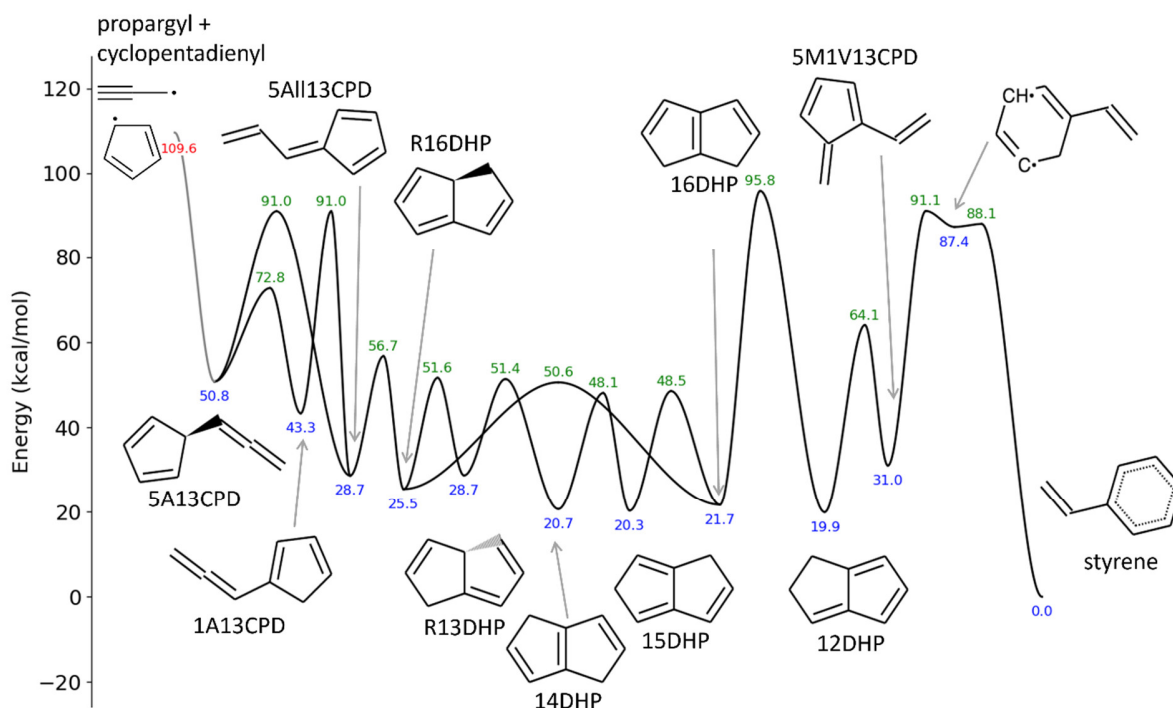


Figure 5: The lowest energy pathway from 5A13CPD [5-(propa-1,2-dien-1-yl)cyclopenta-1,3-diene] to styrene. Energies are calculated at the L3T level and include ZPE.

styrene starts with the adduct via the =C•H end of propargyl, 5-(propa-1,2-dien-1-yl)cyclopenta-1,3-diene (5A13CPD), and leads through cyclopentadiene derivatives (1A13CPD and 5A1113CPD), and dihydropentalene isomers (R13DHP, 14DHP, 15DHP, 16DHP), which are all connected through relatively low barriers with the exception of 1,2-dihydropentalene (12DHP). It is the formation of this latter dihydropentalene species via a 95.8 kcal/mol barrier that “blocks” styrene formation downstream (see discussion below).

The other primary adduct of cyclopentadienyl and propargyl is 5-(prop-2-yn-1-yl)cyclopenta-1,3-diene (5P13CPD). Its isomerization on the C_8H_8 potential energy surface is shown in Fig. 6. Low-energy pathways with submerged barriers exist to form 5-(propa-1,2-dien-1-yl)cyclopenta-1,3-diene (5A13CPD), which was discussed in Fig. 5.

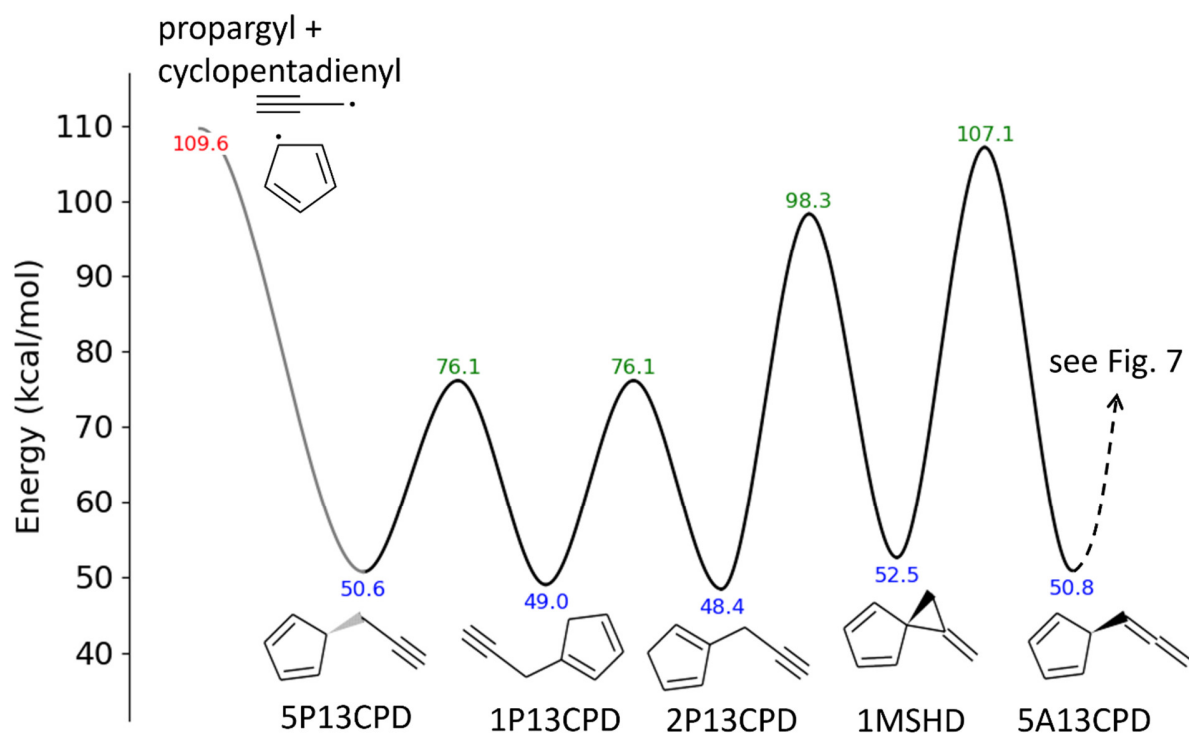
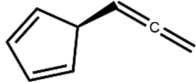
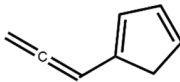
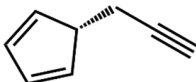
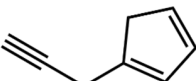
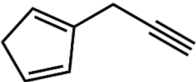
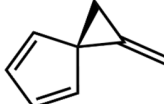
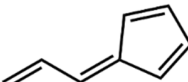
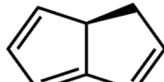
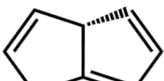
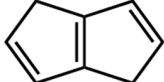
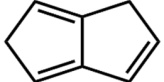
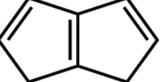
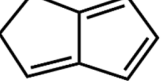
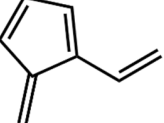


Figure 6: The lowest energy isomerization pathway from 5P13CPD [5-(prop-2-yn-1-yl)cyclopenta-1,3-diene] to 5A13CPD [5-(propa-1,2-dien-1-yl)cyclopenta-1,3-diene]. Energies are calculated at the L3T level and include ZPE.

4.3 The C_8H_8 product identification based on mass-selected threshold photoelectron spectra

In this section, we discuss that the experimentally observed mass-selected threshold photoelectron spectrum for $m/z = 104$ (C_8H_8) can be explained with the presence of most of the isomers that were discussed in the previous section. Except for the dihydropentalenes (DHPs) and styrene, the threshold photoelectron spectra of the relevant species are unknown and had to be simulated as described in Section 3.2. The calculated ionization energies of the various relevant C_8H_8 isomers are listed in Table 1.

Table 1: Ionization energies of various C₈H₈ isomers using the G4 theory.

C ₈ H ₈ isomer structures	Name	Short Name	Calculated AIE / eV
	5-(propa-1,2-dien-1-yl)cyclopenta-1,3-diene	5A13CPD	8.26
	1-(propa-1,2-dien-1-yl)cyclopenta-1,3-diene	1A13CPD	7.68
	5-(prop-2-yn-1-yl)cyclopenta-1,3-diene	5P13CPD	8.54
	1-(prop-2-yn-1-yl)cyclopenta-1,3-diene	1P13CPD	8.30
	2-(prop-2-yn-1-yl)cyclopenta-1,3-diene	2P13CPD	8.34
	1-methylenespiro[2.4]hepta-4,6-diene	1MSHD	8.09
	5-allylidencyclopenta-1,3-diene	5All13CPD	8.03
	(R)-1,6a-dihydropentalene	R16DHP	7.70
	(R)-1,3a-dihydropentalene	R13DHP	8.12
	1,4-dihydropentalene	14DHP	7.51
	1,5-dihydropentalene	15DHP	7.85
	1,6-dihydropentalene	16DHP	7.72
	1,2-dihydropentalene	12DHP	7.81
	5-methylene-1-vinylcyclopenta-1,3-diene	5M1V13CPD	7.79

* from Ref. [77].

The spectrum that needs to be analyzed is shown in Fig. 7 as squared symbols. Several features are identifiable near 7.5, 7.6, 7.7, 7.75, 7.85, and 8.05 eV. The feature in Fig. 7 near 7.5 and 7.6 eV can be assigned to the 1,4-dihydropentalene (14DHP, black, $AIE_{\text{calc},G4} = 7.51$ eV), which exhibits the lowest AIE_{calc} of the C_8H_8 isomers we included in our survey. Based on the calculated ionization energies and simulated photoelectron spectra, most features of the spectrum can be explained, with most prominent assignments depicted in Fig. 7. Besides 14DHP, we assign 1A13CPD [1-(propa-1,2-dien-1-yl)cyclopenta-1,3-diene, cyan, $AIE_{\text{calc},G4} = 7.68$ eV], 16DHP (1,6-dihydropentalene, magenta, $AIE_{\text{calc},G4} = 7.72$ eV), 15DHP (1,5-dihydropentalene, purple, $AIE_{\text{calc},G4} = 7.85$ eV), and 5All13CPD (5-allylidencyclopenta-1,3-diene, orange, $AIE_{\text{calc},G4} = 8.03$ eV),

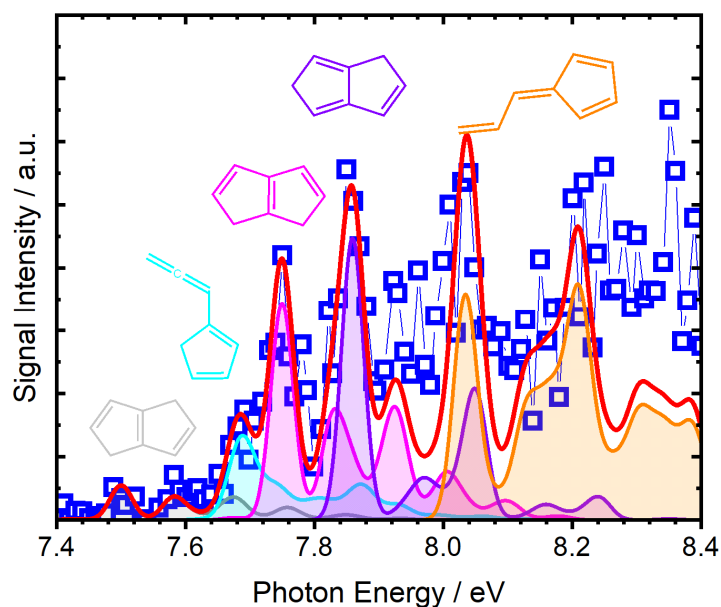


Figure 7: Experimental threshold photoelectron spectrum of $m/z = 104$ (C_8H_8) from the cyclopentadienyl + propargyl reaction (blue squares) in the energy range from 7.4-8.4 eV. Lines and shaded areas represent the simulated photoelectron spectra of five C_8H_8 isomers. The solid red line is the sum of the individual contributions.

respectively, as indicated by the color-coded simulations of their individual Franck-Condon simulations (Fig. 7). The red solid line is the sum of the FC simulations of the five species showing good agreement with most of the features in the experimental ms-TPE spectrum, providing solid spectroscopic evidence for the dihydropentalenes.

It should be mentioned that the 5A13CPD [5-(propa-1,2-dien-1-yl)cyclopenta-1,3-diene] isomer, the initial C₈H₈ isomer that is formed from the recombination of the cyclopentadienyl and the propargyl radical, is likely contributing to the broad spectrum only at around 8.3 eV with a calculated AIE of 8.26 eV (G4). However, the Franck-Condon overlap is small due to extensive structural changes upon ionization, thus leading to an insensitivity towards this particular molecule.

Although most of the pronounced experimental features in Fig. 7 are covered by the FC simulations, discrepancies between experiment and simulations persist, especially above 8.2 eV. It is well known, and also supported by our calculations, that hydrogen atoms in five-membered rings are prone to [1,5]-sigmatropic rearrangement reactions, with barriers of only 25 kcal/mol (Fig. 5) rendering many DHPs accessible. Thus, we improved the missing features by fitting the FC simulations of the remaining DHP isomers to the ms-TPES, as depicted in Fig. 10(a,b).

R16DHP [(R)-1,6a-dihydropentalene, cyan, AIE_{calc,G4} = 7.70 eV], R13DHP [(R)-1,3a-dihydropentalene, magenta, AIE_{calc,G4} = 8.12 eV] and 12DHP (1,2-dihydropentalene, orange, AIE_{calc,G4} = 7.85 eV) can only partially reproduce the missing features in the ms-TPES of *m/z* = 104. This could only be improved by adding the simulation of the fulvene isomer 5M1V13CPD, (5-methylene-1-vinylcyclopenta-1,3-diene, orange AIE_{calc,G4} = 7.79 eV). Nevertheless, contributions from the isomers in Fig. 8(a, b) are likely although spectroscopically challenging to assign due to missing strong transitions partially owed to low FC factors. More importantly, the

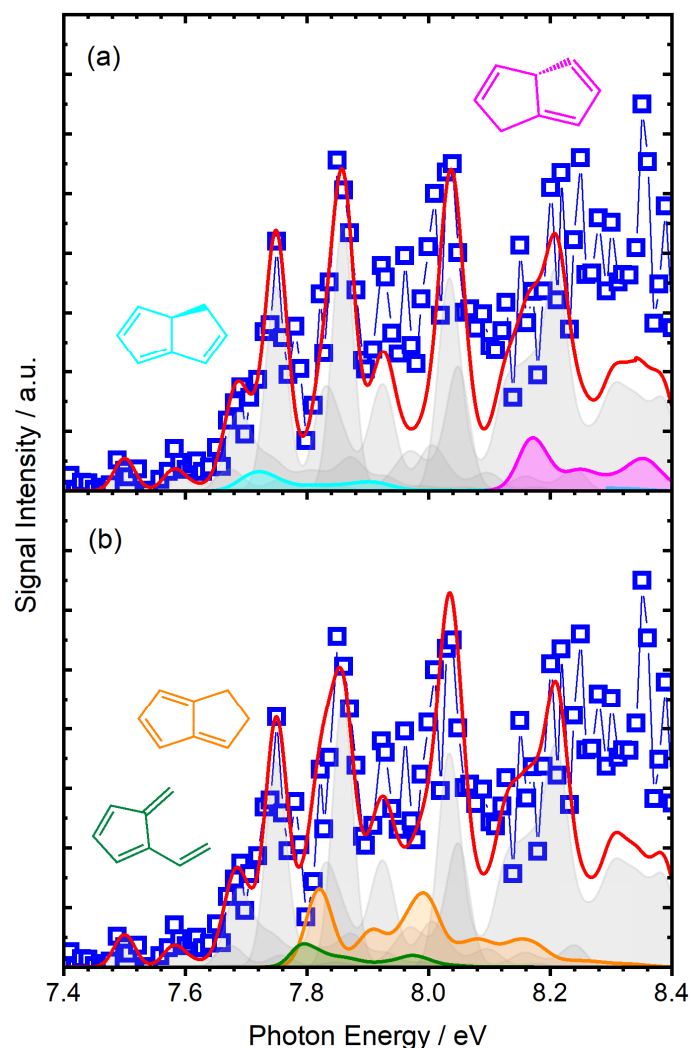


Figure 8: Experimental threshold photoelectron spectrum of $m/z = 104$ (C_8H_8) from the cyclopentadienyl + propargyl reaction (blue squares) in the energy range from 7.4-8.4 eV. Including (a) 1,6a-dihydropentalene and 1,3-dihydropentalene and (b) 5-methylene-1-vinylcyclopenta-1,3-diene and 1,2-dihydropentalene to the fit of the experimental data. Given the overlap with the spectra of the other isomers, the results shown here are at best non-conclusive.

best fit above 8.2 eV was obtained by including the FC simulations of 5P13CPD [5-(prop-2-yn-1-yl)cyclopenta-1,3-diene, green, $AIE_{\text{calc},G4} = 8.54$ eV], 2P13CPD [2-(prop-2-yn-1-yl)cyclopenta-1,3-diene, cyan, $AIE_{\text{calc},G4} = 8.34$ eV] and 5P13CPD [1-(prop-2-yn-1-yl)cyclopenta-1,3-diene, magenta, $AIE_{\text{calc},G4} = 8.30$ eV], as depicted in Fig. 9. Including styrene (not shown here), the most stable isomer of the C_8H_8 potential energy surface, did not increase the overall fit, in agreement

with the reaction network in Fig. 4. Other discussed isomers in this work, such as benzocyclobutene and the xylylenes, could not be identified in the reaction mixture.⁷⁸⁻⁸⁰

Including styrene in the analysis of the experimentally observed near-threshold photoelectron spectrum does not significantly improve the overall agreement between modeled and observed spectra. This is shown in Figs. S4 and S5 of the Supplementary Information. Consequently, the styrene photoelectron spectrum does not support the unambiguous identification of styrene in the C₈H₈ isomer mix, responsible for the observed C₈H₈ threshold photoelectron spectrum.

In summary, we modeled the experimental ms-TPES of the composition C₈H₈ ($m/z = 104$) and the results suggest the appearance of 8 isomers, which all mark minima of the potential energy surface. The contributions of four isomers (as shown in Fig. 8) are not conclusive, given the

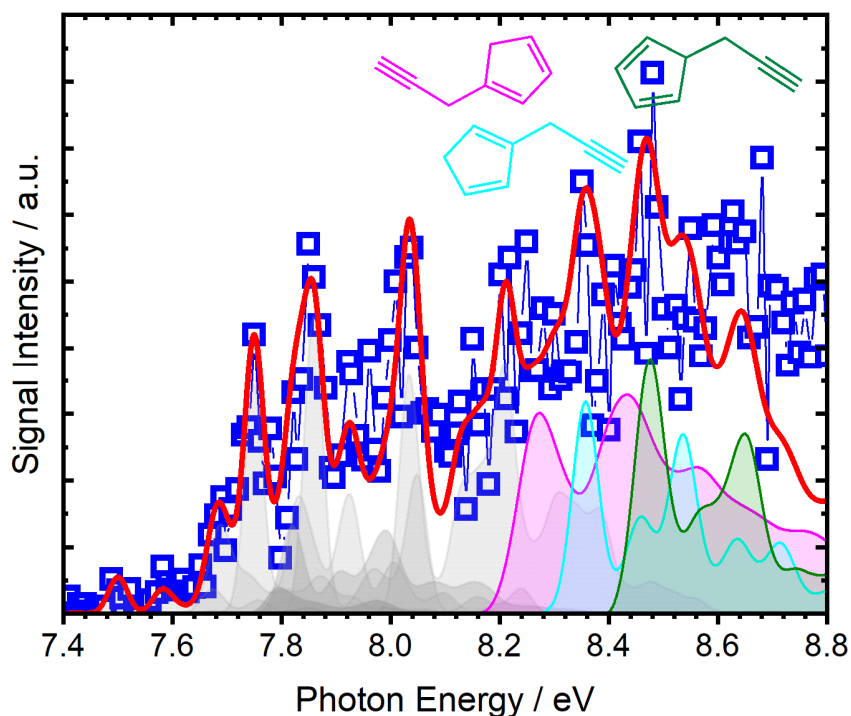


Figure 9: Experimental threshold photoelectron spectrum of $m/z = 104$ (C₈H₈) from the cyclopentadienyl + propargyl reaction (blue squares) in the energy range from 7.4-8.8 eV. Including 5-(prop-2-yn-1-yl)cyclopenta-1,3-diene (green), 2-(prop-2-yn-1-yl)cyclopenta-1,3-diene (cyan), and 1-(prop-2-yn-1-yl)cyclopenta-1,3-diene (magenta) to the fit of the experimental data. Given the overlap with the spectra of the other isomers.

overlapping spectral region with other isomers. Nevertheless, this shows that even complex reaction mixtures, where many isomers contribute, can be successfully disentangled using a combination of well-resolved ms-TPE spectra, Franck-Condon spectral modeling, even in the absence of experimental reference spectra, and a thorough exploration of the potential energy surface.

5. Discussions and Conclusion

Based on the above presented analysis of the mass-selected threshold photoelectron spectra, our experiments clearly show that under the specified experimental conditions, the formation of dihydropentalenes is preferred over the ring-enlargement reaction that forms styrene. This deserves a closer look at the kinetics on the C_8H_8 PES.

Our calculations suggest that the formation of styrene is controlled by the high and tight barrier at 95.8 kcal/mol (see Fig. 5). However, this barrier is in principle surmountable given the energy of reactants (109.6 kcal/mol), and thus styrene formation cannot simply be excluded. Instead, we need to compare styrene formation to competing reactions. Besides the reactions shown in Fig. 5, dihydropentalenes can lose H atoms, leading to one of the two possible resonantly stabilized C_8H_7 radicals with the same backbone as that of the dihydropentalenes, see Fig. 8. Since these H-loss reactions are likely barrierless and are within 1 kcal/mol of the tight bottleneck barrier, they can effectively compete with isomerization.

To place an upper limit on the yield of styrene, we set up a very simple master equation model. We only considered the two dihydropentalene wells on the two sides of the isomerization barrier, the one at 21.7 kcal/mol and the other at 19.9 kcal/mol (see Fig. 10, species 16DHP and 12DHP, respectively). In the model we connected the lower energy H-loss product at 95.1 kcal/mol directly

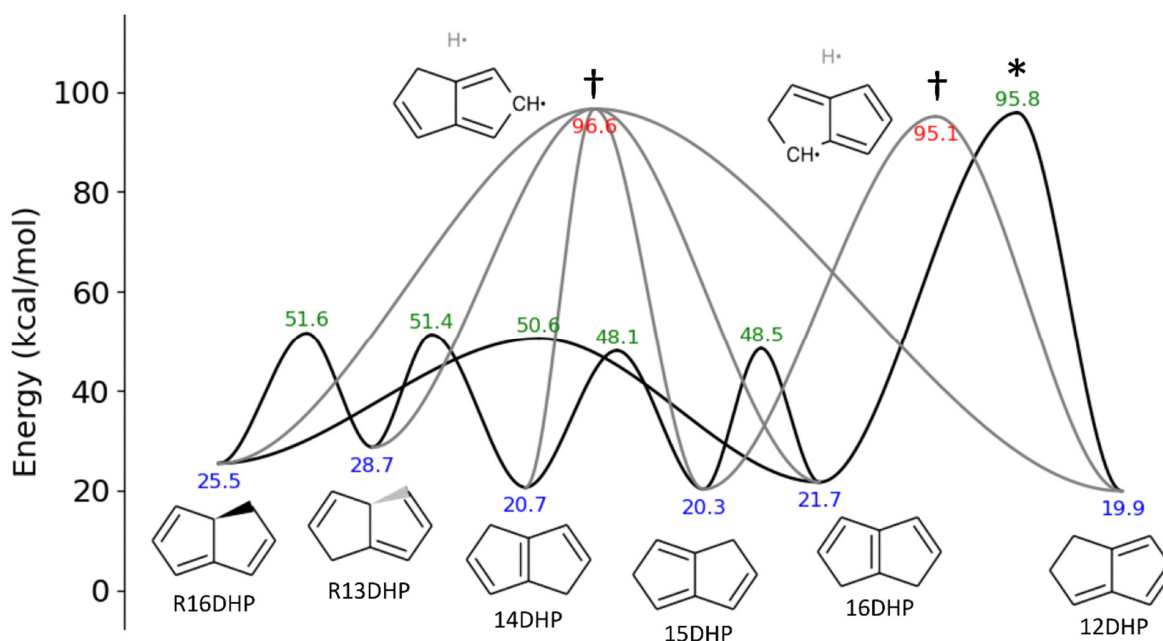


Figure 10: Part of the C_8H_8 PES showing the bottleneck barrier towards styrene (marked with an *) connecting species A and B, and the H loss channels forming bimolecular bridges (marked with †). The H loss product included in the simple master equation model is marked as C.

to well 16DHP, because the dihydropentalenes prior to the high barrier between 16DHP and 12DHP (marked with *) are expected to equilibrate much faster than dissociation or isomerization. We also assumed that cyclopentadienyl + propargyl forms species 16DHP directly, essentially saying that at the experimental conditions the saddles between the entrance and species 16DHP play no role in the system's propensity to form styrene. We assigned a capture rate coefficient of $3 \times 10^{-11} \text{ cm}^3 \text{ molecule}^{-1} \text{ s}^{-1}$ to cyclopentadienyl + propargyl, in analogy to the self-reaction of propargyl and of cyclopentadienyl around 1100 K.^{81, 82} Finally, we assumed that the capture rate coefficient of the H + radical reaction is $4 \times 10^{-10} \text{ cm}^3 \text{ molecule}^{-1} \text{ s}^{-1}$, in analogy to the propargyl +

H capture rate coefficient.⁸³ Representing the barrierless processes with phase-space theory as implemented in MESS,^{69, 70} we calculated rate coefficients for our model system thus consisting of bimolecular species cyclopentadienyl + propargyl and the lower H + C₈H₇, and wells 16DHP and 12DHP. The MESS input file is included in the SI.

Our calculations show that at 20 Torr and 1150 K about 80% of the cyclopentadienyl + propargyl reactants get stabilized in well 16DHP, 20% escapes through the H + C₈H₇ bimolecular exit, and only 0.05% goes from the reactants to 12DHP in a well-skipping process. The unimolecular reactions of the stabilized 16DHP also yield only about 0.05% 12DHP, capping the yield of styrene. Considering that there are six low-lying channels for H loss before surmounting the tight barrier, the true branching towards styrene is expected to be even lower. We can, therefore, conclude that in accordance with the experiments isomerization towards styrene is not competitive, and thus styrene is expected to be a minor product with an upper limit of 0.05% under our conditions. Note, however, that under certain conditions (such as high H atom concentration), the reverse of these H-loss channels can become bimolecular bridges leading the isolated dihydropentalene without the need to overcome the tight barrier.⁴¹

Note also that the Sharma *et al.* bottleneck barrier is looser than the one found in this work. The rate coefficient at 1050 K through the Sharma *et al.* barrier is 18% of the relative to the rate coefficient of our new bottleneck, and around 1500 K the two barriers create equal bottlenecks. The Sharma *et al.* barrier dominates by ~5.5x at 2500 K. This, however, does not impact the finding of the paper that styrene formation is a minor channel around 1050 K.

The results presented here have interesting implications on our understanding of molecular-weight growth mechanisms. The importance of styrene formation at combustion conditions through ring-enlargement after the reaction of cyclopentadienyl with propargyl is likely to be

limited. Since stabilization in the various dihydropentalene wells dominate at low pressures of 20-30 Torr, it can be expected to be even more important at relevant pressures, *i.e.*, atmospheric pressure and above. This conclusion may change when going to higher experimental temperatures, however, for combustion environments, we noted that contributions of C₅H₅ are generally limited due its decomposition into propargyl and acetylene. Also, as pointed out above, the importance of styrene formation through reaction (R1) is limited by competing with the formation of C₈H₇ dihydropentalenyl radical species, that technically are formed through radical-radical chain reactions as proposed by Johansson *et al.*⁸⁴ Consistent with earlier work,²¹ we also found here that the stabilization of the closed-shell species (C₈H₈ in this study) dominates over the radical + H channel. There is nothing known about the stability of the various C₈H₇ radicals under these conditions, but it might be that they undergo ring-opening or lose another H to form C₈H₆. Hydrogen (H₂) loss from 12DHP, the DHP that has neighboring extra H-atoms, is a possibility for subsequent C₈H₈ reactions. The barrier is 95.3 kcal/mol, which is comparable to H-loss channels from DHPs, but the transition state is tight, so the reaction is expected to be slow. Further work describing the kinetics on the C₈H₈ potential energy surface is needed to unravel the importance of these processes quantitatively.

Dihydropentalenes (DHPs) have not been identified as soot precursors and are not included in up-to-date mechanisms. Thus, the specific role of DHPs in the overall molecular-weight growth processes is less clear than the role of PAHs. However, the structural and chemical characteristics of DHPs suggests that they could play a role. For example, can the reaction of dihydropentalenyl radicals with methyl radicals lead to the formation of indene in a ring-enlargement reaction analogue to fulvene/benzene formation through the cyclopentadienyl+CH₃ reaction?¹⁹

Styrene, the most stable C₈H₈ isomers, has been identified in many flame studies. However, the ring-enlargement reaction of C₅H₅ + C₃H₃ is not its only formation pathway that has been identified in modeling work. The bicyclic structure of DHPs and their potential for further cyclization and growth make them plausible candidates for participation in the soot formation process. The importance of dihydropentalenes for molecular-weight growth should be tested in flame models using a comprehensive chemical kinetic mechanism. We expect that DHPs can serve as fundamental building blocks for constructing more complex carbon nanostructures and that their unique ring systems can be incorporated into larger molecular frameworks.

AUTHOR INFORMATION

Corresponding Author

*Corresponding author: nhansen@sandia.gov; (925) 294-6272

Author Contributions

The manuscript was written through contributions of all authors. All authors have given approval to the final version of the manuscript.

Supplementary Information:

Supplementary information is available. It contains (1) information about the C₅H₅ and C₃H₃ identification, (2) the description of the process to reduce the large PES, (3) the interactive version of Figure 4, (4) the input file to the PESViewer, (5) the MESS input file, (6) the simulated threshold photoelectron spectrum for $m/z = 104$ including styrene, (7) the Cartesian coordinates of all structures shown in Figure 4, (8) the discussion of the Sharma *et al.* bottleneck, and (9) the high-pressure rate constants.

Acknowledgments

NH and JZ are supported by the Gas-Phase Chemical Physics program of the US Department of Energy, Office of Science, Office of Basic Energy Science, Division of Chemical Sciences, Geosciences and Biosciences. NH was also supported by the Helmholtz Association through a Helmholtz International Fellow Award. The experiments were performed at the VUV (x04db) beamline of the Swiss Light Source (SLS) located at Paul Scherrer Institute (PSI), Villigen, Switzerland. The authors are grateful to Hannes Lüdtke and Patrick Ascher (PSI) for supporting the measurement campaign. Sandia National Laboratories is a multimission laboratory managed and operated by the National Technology and Engineering Solutions of Sandia, LLC, a wholly owned subsidiary of Honeywell International, Inc., for the U.S. DOE's National Nuclear Security Administration under contract DENA0003525. This paper describes objective technical results and analysis. Any subjective views or opinions that might be expressed in the paper do not necessarily represent the views of the U.S. DOE or the U.S. Government.

References

- (1) Bockhorn, H.; D'Anna, A.; Sarofim, A. F.; Wang, H. Combustion generated fine carbonaceous particles. KIT Scientific publishing: 2014.
- (2) Kaiser, R. I.; Hansen, N. An aromatic universe – A physical chemistry perspective. *The Journal of Physical Chemistry A* **2021**, *125* (18), 3826-3840.
- (3) Martin, J. W.; Salamanca, M.; Kraft, M. Soot inception: Carbonaceous nanoparticle formation in flames. *Progress in Energy and Combustion Science* **2022**, *88*, 100956.
- (4) Wang, H. Formation of nascent soot and other condensed-phase materials in flames. *Proceedings of the Combustion Institute* **2011**, *33* (1), 41-67.
- (5) Frenklach, M.; Mebel, A. M. On the mechanism of soot nucleation. *Physical Chemistry Chemical Physics* **2020**, *22* (9), 5314-5331.
- (6) Ali, M. U.; Siyi, L.; Yousaf, B.; Abbas, Q.; Hameed, R.; Zheng, C.; Kuang, X.; Wong, M. H. Emission sources and full spectrum of health impacts of black carbon associated polycyclic aromatic hydrocarbons (PAHs) in urban environment: A review. *Critical Reviews in Environmental Science and Technology* **2021**, *51* (9), 857-896.
- (7) Mallah, M. A.; Changxing, L.; Mallah, M. A.; Noreen, S.; Liu, Y.; Saeed, M.; Xi, H.; Ahmed, B.; Feng, F.; Mirjat, A. A.; et al. Polycyclic aromatic hydrocarbon and its effects on human health: An overview. *Chemosphere* **2022**, *296*, 133948.
- (8) Teoh, R.; Engberg, Z.; Schumann, U.; Voigt, C.; Shapiro, M.; Rohs, S.; Stettler, M. E. Global aviation contrail climate effects from 2019 to 2021. *Atmospheric Chemistry and Physics* **2024**, *24* (10), 6071-6093.
- (9) Lee, D. S.; Fahey, D. W.; Skowron, A.; Allen, M. R.; Burkhardt, U.; Chen, Q.; Doherty, S. J.; Freeman, S.; Forster, P. M.; Fuglestedt, J. The contribution of global aviation to anthropogenic climate forcing for 2000 to 2018. *Atmospheric Environment* **2021**, *244*, 117834.
- (10) Hansen, N.; Miller, J. A.; Klippenstein, S. J.; Westmoreland, P. R.; Kohse-Höinghaus, K. Exploring formation pathways of aromatic compounds in laboratory-based model flames of aliphatic fuels. *Combustion, Explosion, and Shock Waves* **2012**, *48*, 508-515.
- (11) Miller, J. A.; Klippenstein, S. J. The recombination of propargyl radicals and other reactions on a C₆H₆ potential. *The Journal of Physical Chemistry A* **2003**, *107* (39), 7783-7799.

- (12) Zhao, L.; Lu, W.; Ahmed, M.; Zagidullin, M. V.; Azyazov, V. N.; Morozov, A. N.; Mebel, A. M.; Kaiser, R. I. Gas-phase synthesis of benzene via the propargyl radical self-reaction. *Science Advances* **2021**, 7 (21), eabf0360.
- (13) Hrodmarsson, H. R.; Garcia, G. A.; Bourehil, L.; Nahon, L.; Gans, B.; Boyé-Péronne, S.; Guillemin, J.-C.; Loison, J.-C. The isomer distribution of C₆H₆ products from the propargyl radical gas-phase recombination investigated by threshold-photoelectron spectroscopy. *Communications Chemistry* **2024**, 7 (1), 156.
- (14) Miller, J. A.; Klippenstein, S. J.; Georgievskii, Y.; Harding, L. B.; Allen, W. D.; Simmonett, A. C. Reactions between resonance-stabilized radicals: propargyl+ allyl. *The Journal of Physical Chemistry A* **2010**, 114 (14), 4881-4890.
- (15) Hansen, N.; Li, W.; Law, M. E.; Kasper, T.; Westmoreland, P. R.; Yang, B.; Cool, T. A.; Lucassen, A. The importance of fuel dissociation and propargyl+ allyl association for the formation of benzene in a fuel-rich 1-hexene flame. *Physical Chemistry Chemical Physics* **2010**, 12 (38), 12112-12122.
- (16) Hansen, N.; Miller, J. A.; Kasper, T.; Kohse-Höinghaus, K.; Westmoreland, P. R.; Wang, J.; Cool, T. A. Benzene formation in premixed fuel-rich 1, 3-butadiene flames. *Proceedings of the Combustion Institute* **2009**, 32 (1), 623-630.
- (17) Senosiain, J. P.; Miller, J. A. The reaction of n- and i-C₄H₅ radicals with acetylene. *The Journal of Physical Chemistry A* **2007**, 111 (19), 3740-3747.
- (18) Hansen, N.; Klippenstein, S. J.; Taatjes, C. A.; Miller, J. A.; Wang, J.; Cool, T. A.; Yang, B.; Yang, R.; Wei, L.; Huang, C. Identification and chemistry of C₄H₃ and C₄H₅ isomers in fuel-rich flames. *The Journal of Physical Chemistry A* **2006**, 110 (10), 3670-3678.
- (19) Kaiser, R. I.; Zhao, L.; Lu, W.; Ahmed, M.; Zagidullin, M. V.; Azyazov, V. N.; Mebel, A. M. Formation of benzene and naphthalene through cyclopentadienyl-mediated radical-radical reactions. *The Journal of Physical Chemistry Letters* **2021**, 13 (1), 208-213.
- (20) Baroncelli, M.; Mao, Q.; Galle, S.; Hansen, N.; Pitsch, H. Role of ring-enlargement reactions in the formation of aromatic hydrocarbons. *Physical Chemistry Chemical Physics* **2020**, 22 (8), 4699-4714.
- (21) Couch, D. E.; Kukkadapu, G.; Zhang, A. J.; Jasper, A. W.; Taatjes, C. A.; Hansen, N. The role of radical-radical chain-propagating pathways in the phenyl + propargyl reaction. *Proceedings of the Combustion Institute* **2023**, 39 (1), 643-651.

- (22) Hansen, N.; Bierkandt, T.; Gaiser, N.; Oßwald, P.; Köhler, M.; Hemberger, P. Formation of five-membered ring structures via reactions of *o*-benzyne. *Proceedings of the Combustion institute* **2024**, *40* (1-4), 105623.
- (23) Selby, T. M.; Goulay, F.; Soorkia, S.; Ray, A.; Jasper, A. W.; Klippenstein, S. J.; Morozov, A. N.; Mebel, A. M.; Savee, J. D.; Taatjes, C. A. Radical–radical reactions in molecular weight growth: The phenyl+ propargyl reaction. *The Journal of Physical Chemistry A* **2023**, *127* (11), 2577-2590.
- (24) Kislov, V.; Mebel, A. Ab initio G3-type/statistical theory study of the formation of indene in combustion flames. I. Pathways involving benzene and phenyl radical. *The Journal of Physical Chemistry A* **2007**, *111* (19), 3922-3931.
- (25) Lindstedt, P.; Maurice, L.; Meyer, M. Thermodynamic and kinetic issues in the formation and oxidation of aromatic species. *Faraday discussions* **2002**, *119*, 409-432.
- (26) Morozov, A. N.; Mebel, A. M. Theoretical study of the reaction mechanism and kinetics of the phenyl+propargyl association. *Physical Chemistry Chemical Physics* **2020**, *22* (13), 6868-6880.
- (27) Cavallotti, C.; Polino, D.; Frassoldati, A.; Ranzi, E. Analysis of some reaction pathways active during cyclopentadiene pyrolysis. *The Journal of Physical Chemistry A* **2012**, *116* (13), 3313-3324.
- (28) Djokic, M. R.; Van Geem, K. M.; Cavallotti, C.; Frassoldati, A.; Ranzi, E.; Marin, G. B. An experimental and kinetic modeling study of cyclopentadiene pyrolysis: First growth of polycyclic aromatic hydrocarbons. *Combustion and Flame* **2014**, *161* (11), 2739-2751.
- (29) Fascella, S.; Cavallotti, C.; Rota, R.; Carrà, S. The peculiar kinetics of the reaction between acetylene and the cyclopentadienyl radical. *The Journal of Physical Chemistry A* **2005**, *109* (33), 7546-7557.
- (30) Mao, Q.; Huang, C.; Baroncelli, M.; Shen, L.; Cai, L.; Leonhard, K.; Pitsch, H. Unimolecular reactions of the resonance-stabilized cyclopentadienyl radicals and their role in the polycyclic aromatic hydrocarbon formation. *Proceedings of the Combustion Institute* **2021**, *38* (1), 729-737.
- (31) Melius, C. F.; Colvin, M. E.; Marinov, N. M.; Pit, W. J.; Senkan, S. M. Reaction mechanisms in aromatic hydrocarbon formation involving the C₅H₅ cyclopentadienyl moiety. In *Symposium (International) on Combustion*, 1996; Elsevier: Vol. 26, pp 685-692.
- (32) Mulholland, J. A.; Lu, M.; Kim, D.-H. Pyrolytic growth of polycyclic aromatic hydrocarbons by cyclopentadienyl moieties. *Proceedings of the Combustion Institute* **2000**, *28* (2), 2593-2599.

- (33) Kern, R. D.; Zhang, Q.; Yao, J.; Jursic, B. S.; Tranter, R. S.; Greybill, M. A.; Kiefer, J. H. Pyrolysis of cyclopentadiene: Rates for initial C–H bond fission and the decomposition of c-C₅H₅. *Symposium (International) on Combustion* **1998**, 27 (1), 143-150.
- (34) Martí, C.; Devereux, C.; Najm, H. N.; Zádor, J. Evaluation of rate coefficients in the gas phase using machine-learned potentials. *The Journal of Physical Chemistry A* **2024**, 128 (10), 1958-1971.
- (35) Hansen, N.; Kasper, T.; Klippenstein, S. J.; Westmoreland, P. R.; Law, M. E.; Taatjes, C. A.; Kohse-Höinghaus, K.; Wang, J.; Cool, T. A. Initial steps of aromatic ring formation in a laminar premixed fuel-rich cyclopentene flame. *The Journal of Physical Chemistry A* **2007**, 111 (19), 4081-4092.
- (36) Bierkandt, T.; Hemberger, P.; Oßwald, P.; Krüger, D.; Köhler, M.; Kasper, T. Flame structure of laminar premixed anisole flames investigated by photoionization mass spectrometry and photoelectron spectroscopy. *Proceedings of the Combustion Institute* **2019**, 37 (2), 1579-1587.
- (37) Jasper, A. W.; Hansen, N. Hydrogen-assisted isomerizations of fulvene to benzene and of larger cyclic aromatic hydrocarbons. *Proceedings of the Combustion Institute* **2013**, 34 (1), 279-287.
- (38) Zhao, L.; Kaiser, R. I.; Lu, W.; Xu, B.; Ahmed, M.; Morozov, A. N.; Mebel, A. M.; Howlader, A. H.; Wnuk, S. F. Molecular mass growth through ring expansion in polycyclic aromatic hydrocarbons via radical–radical reactions. *Nature Communications* **2019**, 10 (1), 3689.
- (39) Cavallotti, C.; Mancarella, S.; Rota, R.; Carrà, S. Conversion of C₅ into C₆ cyclic species through the formation of C₇ intermediates. *The Journal of Physical Chemistry A* **2007**, 111 (19), 3959-3969.
- (40) Cavallotti, C.; Polino, D. On the kinetics of the C₅H₅+C₅H₅ reaction. *Proceedings of the Combustion Institute* **2013**, 34 (1), 557-564.
- (41) Martí, C.; Michelsen, H. A.; Najm, H. N.; Zádor, J. Comprehensive kinetics on the C₇H₇ potential energy surface under combustion conditions. *The Journal of Physical Chemistry A* **2023**, 127 (8), 1941-1959.
- (42) Sharma, S.; Harper, M. R.; Green, W. H. Modeling of 1, 3-hexadiene, 2, 4-hexadiene and 1, 4-hexadiene-doped methane flames: Flame modeling, benzene and styrene formation. *Combustion and Flame* **2010**, 157 (7), 1331-1345.
- (43) Dudek, D.; Glänzer, K.; Troe, J. Pyrolysis of 1.3.5.7-cyclooctatetraene, semibullvalene, and 1.5-dihydropentalene in shock waves and in a flow system (Part I). *Berichte der Bunsengesellschaft für Physikalische Chemie* **1979**, 83 (8), 776-788.

- (44) Hassenrueck, K.; Martin, H. D.; Walsh, R. Consequences of strain in (CH)₈ hydrocarbons. *Chemical Reviews* **1989**, *89* (5), 1125-1146.
- (45) Jones, M., Jr.; Schwab, L. O. The cyclooctatetraene-dihydropentalene rearrangement. *Journal of the American Chemical Society* **1968**, *90* (23), 6549-6550.
- (46) Karton, A.; Martin, J. M. Explicitly correlated benchmark calculations on C₈H₈ isomer energy separations: how accurate are DFT, double-hybrid, and composite ab initio procedures? *Molecular Physics* **2012**, *110* (19-20), 2477-2491.
- (47) Li, Z.; Anderson, S. L. Pyrolysis chemistry of cubane and methylcubane: The effect of methyl substitution on stability and product branching. *The Journal of Physical Chemistry A* **2003**, *107* (8), 1162-1174.
- (48) Martin, H.; Urbanek, T.; Walsh, R. Thermal behavior of C₈H₈ hydrocarbons. 2. Semibullvalene: kinetic and thermodynamic stability. *Journal of the American Chemical Society* **1985**, *107* (19), 5532-5534.
- (49) Martin, H. D.; Urbanek, T.; Braun, R.; Walsh, R. The kinetics of pyrolysis of barrelene [1]: A concerted process on the C₈H₈ energy surface. *International Journal of Chemical Kinetics* **1984**, *16* (2), 117-124.
- (50) Hemberger, P.; Bodi, A.; Bierkandt, T.; Köhler, M.; Kaczmarek, D.; Kasper, T. Photoelectron photoion coincidence spectroscopy provides mechanistic insights in fuel synthesis and conversion. *Energy & Fuels* **2021**, *35* (20), 16265-16302.
- (51) Hemberger, P.; Pan, Z.; Wu, X.; Zhang, Z.; Kanayama, K.; Bodi, A. Photoion mass-selected threshold photoelectron spectroscopy to detect reactive intermediates in catalysis: From instrumentation and examples to peculiarities and a database. *The Journal of Physical Chemistry C* **2023**, *127* (34), 16751-16763.
- (52) Van de Vijver, R.; Zádor, J. KinBot: Automated stationary point search on potential energy surfaces. *Computer Physics Communications* **2020**, *248*, 106947.
- (53) Zádor, J.; Martí, C.; Van de Vijver, R.; Johansen, S. L.; Yang, Y.; Michelsen, H. A.; Najm, H. N. Automated reaction kinetics of gas-phase organic species over multiwell potential energy surfaces. *The Journal of Physical Chemistry A* **2023**, *127* (3), 565-588.
- (54) Couch, D.; San Marchi, M. M.; Hansen, N. Experimental observation of molecular-weight growth by the reactions of o-benzyne with benzyl radicals. *Physical Chemistry Chemical Physics* **2024**, *26*, 24833-24840.

- (55) Couch, D. E.; Jasper, A. W.; Kukkadapu, G.; San Marchi, M. M.; Zhang, A. J.; Taatjes, C. A.; Hansen, N. Molecular-weight growth by the phenyl+cyclopentadienyl reaction: Well-skipping and ring-opening. *Combustion and Flame* **2023**, *257*, 112439.
- (56) Couch, D. E.; Zhang, A. J.; Taatjes, C. A.; Hansen, N. Experimental observation of hydrocarbon growth by resonance-stabilized radical–radical chain reaction. *Angewandte Chemie International Edition* **2021**, *60* (52), 27230-27235.
- (57) Li, W.; Yang, J.; Zhao, L.; Couch, D.; Marchi, M. S.; Hansen, N.; Morozov, A. N.; Mebel, A. M.; Kaiser, R. I. Gas-phase preparation of azulene (C₁₀H₈) and naphthalene (C₁₀H₈) via the reaction of the resonantly stabilized fulvenallenyl (C₇H₅[•]) and propargyl (C₃H₃[•]) radicals. *Chemical Science* **2023**, *14* (36), 9795-9805.
- (58) Kohn, D. W.; Clauberg, H.; Chen, P. Flash pyrolysis nozzle for generation of radicals in a supersonic jet expansion. *Review of Scientific Instruments* **1992**, *63* (8), 4003-4005.
- (59) Guan, Q.; Urness, K. N.; Ormond, T. K.; David, D. E.; Barney Ellison, G.; Daily, J. W. The properties of a micro-reactor for the study of the unimolecular decomposition of large molecules. *International Reviews in Physical Chemistry* **2014**, *33* (4), 447-487.
- (60) Sztáray, B.; Voronova, K.; Torma, K. G.; Covert, K. J.; Bodi, A.; Hemberger, P.; Gerber, T.; Osborn, D. L. CRF-PEPICO: Double velocity map imaging photoelectron photoion coincidence spectroscopy for reaction kinetics studies. *The Journal of Chemical Physics* **2017**, *147* (1), 013944.
- (61) Baer, T.; Tuckett, R. P. Advances in threshold photoelectron spectroscopy (TPES) and threshold photoelectron photoion coincidence (TPEPICO). *Physical Chemistry Chemical Physics* **2017**, *19* (15), 9698-9723.
- (62) Johnson, M.; Bodi, A.; Schulz, L.; Gerber, T. Vacuum ultraviolet beamline at the Swiss Light Source for chemical dynamics studies. *Nucl. Instrum. Methods Phys. Res.* **2009**, *610* (2), 597-603.
- (63) Bodi, A.; Sztáray, B.; Baer, T.; Johnson, M.; Gerber, T. Data acquisition schemes for continuous two-particle time-of-flight coincidence experiments. *Review of Scientific Instruments* **2007**, *78* (8), 084102.
- (64) Sztáray, B.; Baer, T. Suppression of hot electrons in threshold photoelectron photoion coincidence spectroscopy using velocity focusing optics. *Review of Scientific Instruments* **2003**, *74* (8), 3763-3768.
- (65) Sheps, L.; Dewyer, A. L.; Demireva, M.; Zádor, J. Quantitative detection of products and radical intermediates in low-temperature oxidation of cyclopentane. *The Journal of Physical Chemistry A* **2021**, *125* (20), 4467-4479.

(66) Frisch, M. J.; Trucks, G. W.; Schlegel, H. B.; Scuseria, G. E.; Robb, M. A.; Cheeseman, J. R.; Scalmani, G.; Barone, V.; Petersson, G. A.; Nakatsuji, H.; et al., *Gaussian 16 Rev. C.02*; Wallingford, CT, 2016.

(67) Werner, H. J.; Knowles, P. J.; Celani, P.; Györffy, W.; Hesselmann, A.; Kats, D.; Knizia, G.; Köhn, A.; Korona, T.; Kreplin, D.; et al., *MOLPRO, version 2022, a package of ab initio programs*; www.molpro.net, 2022.

(68) van de Vijver, R., *PESViewer*; 2019. <https://github.com/rubenvdvijver/PESViewer?tab=readme-ov-file>.

(69) Georgievskii, Y.; Klippenstein, S. J., *MESS.2016.3.23.*; 2016. <https://tcg.cse.anl.gov/papr/codes/mess.html>.

(70) Georgievskii, Y.; Miller, J. A.; Burke, M. P.; Klippenstein, S. J. Reformulation and solution of the master equation for multiple-well chemical reactions. *The Journal of Physical Chemistry A* **2013**, *117* (46), 12146-12154.

(71) Friderichsen, A. V.; Shin, E.-J.; Evans, R. J.; Nimlos, M. R.; Dayton, D. C.; Ellison, G. B. The pyrolysis of anisole (C₆H₅OCH₃) using a hyperthermal nozzle. *Fuel* **2001**, *80* (12), 1747-1755.

(72) Pecullan, M.; Brezinsky, K.; Glassman, I. Pyrolysis and oxidation of anisole near 1000 K. *The Journal of Physical Chemistry A* **1997**, *101* (18), 3305-3316.

(73) Yuan, W.; Li, T.; Li, Y.; Zeng, M.; Zhang, Y.; Zou, J.; Cao, C.; Li, W.; Yang, J.; Qi, F. Experimental and kinetic modeling investigation on anisole pyrolysis: Implications on phenoxy and cyclopentadienyl chemistry. *Combustion and Flame* **2019**, *201*, 187-199.

(74) Zhang, T.; Bhattarai, C.; Son, Y.; Samburova, V.; Khlystov, A.; Varganov, S. A. Reaction mechanisms of anisole pyrolysis at different temperatures: Experimental and theoretical studies. *Energy & Fuels* **2021**, *35* (12), 9994-10008.

(75) Fernholz, C.; Bodi, A.; Hemberger, P. Threshold photoelectron spectrum of the phenoxy radical. *The Journal of Physical Chemistry A* **2022**, *126* (48), 9022-9030.

(76) Maier, J.; Turner, D. Steric inhibition of resonance studied by molecular photoelectron spectroscopy. Part 3.—Anilines, phenols and related compounds. *Journal of the Chemical Society, Faraday Transactions 2: Molecular and Chemical Physics* **1973**, *69*, 521-531.

(77) Dyke, J. M.; Ozeki, H.; Takahashi, M.; Cockett, M. C. R.; Kimura, K. A study of phenylacetylene and styrene, and their argon complexes PA-Ar and ST-Ar with laser threshold photoelectron spectroscopy. *The Journal of Chemical Physics* **1992**, *97* (12), 8926-8933.

(78) Steglich, M.; Custodis, V. B. F.; Trevitt, A. J.; daSilva, G.; Bodi, A.; Hemberger, P. Photoelectron spectrum and energetics of the meta-xylylene diradical. *Journal of the American Chemical Society* **2017**, *139* (41), 14348-14351.

(79) Hemberger, P.; Trevitt, A. J.; Gerber, T.; Ross, E.; da Silva, G. Isomer-specific product detection of gas-phase xylyl radical rearrangement and decomposition using VUV synchrotron photoionization. *The Journal of Physical Chemistry A* **2014**, *118* (20), 3593-3604.

(80) Hemberger, P.; Trevitt, A. J.; Ross, E.; da Silva, G. Direct observation of para-xylylene as the decomposition product of the meta-xylyl radical using VUV synchrotron radiation. *The Journal of Physical Chemistry Letters* **2013**, *4* (15), 2546-2550.

(81) Georgievskii, Y.; Miller, J. A.; Klippenstein, S. J. Association rate constants for reactions between resonance-stabilized radicals: $C_3H_3 + C_3H_3$, $C_3H_3 + C_3H_5$, and $C_3H_5 + C_3H_5$. *Physical Chemistry Chemical Physics* **2007**, *9* (31), 4259-4268.

(82) Knyazev, V. D.; Popov, K. V. Kinetics of the self reaction of cyclopentadienyl radicals. *The Journal of Physical Chemistry A* **2015**, *119* (28), 7418-7429.

(83) Harding, L. B.; Klippenstein, S. J.; Georgievskii, Y. On the combination reactions of hydrogen atoms with resonance-stabilized hydrocarbon radicals. *The Journal of Physical Chemistry A* **2007**, *111* (19), 3789-3801.

(84) Johansson, K. O.; Head-Gordon, M. P.; Schrader, P. E.; Wilson, K. R.; Michelsen, H. A. Resonance-stabilized hydrocarbon-radical chain reactions may explain soot inception and growth. *Science* **2018**, *361* (6406), 997-1000.